Applied Catalysis B: Environmental 168-169 (2015) 370–376

Contents lists available at ScienceDirect

Applied Catalysis B: Environmental

journal homepage: www.elsevier.com/locate/apcatb

Dual function materials for CO_2 capture and conversion using renewable H_2

Melis S. Duyar[a], Martha A. Arellano Treviño[b], Robert J. Farrauto[a,*]

[a] Earth and Environmental Engineering Department, Columbia University in the City of New York, 500 W 120th Street, New York, NY 10027, United States
[b] Chemical Engineering Department, Columbia University in the City of New York, 500 W 120th Street, New York, NY 10027, United States

ARTICLE INFO

Article history:
Received 7 November 2014
Received in revised form
16 December 2014
Accepted 17 December 2014
Available online 8 January 2015

Keywords:
Carbon neutrality
CO_2 capture
CO_2 utilization
Methanation
CO_2 adsorption
RuCaO/γ-Al_2O_3
Dual function material

ABSTRACT

The accumulation of CO_2 emissions in the atmosphere due to industrialization is being held responsible for climate change with increasing certainty by the scientific community. In order to prevent its further accumulation in the atmosphere, CO_2 must be captured for storage or converted to useful products. Current materials and processes for CO_2 capture are energy intensive. We report a feasibility study of dual function materials (DFM), which capture CO_2 from an emission source and at the same temperature (320 °C) in the same reactor convert it to synthetic natural gas, requiring no additional heat input. The DFM consists of Ru as methanation catalyst and nano dispersed CaO as CO_2 adsorbent, both supported on a porous γ-Al_2O_3 carrier. A spillover process drives CO_2 from the sorbent to the Ru sites where methanation occurs using stored H_2 from excess renewable power. This approach utilizes flue gas sensible heat and eliminates the current energy intensive and corrosive capture and storage processes without having to transport captured CO_2 or add external heat.

1. Introduction

Given the growing world population, which naturally translates to a growing energy demand, successful energy strategies of the future will have to focus on securing energy while making significant decreases in greenhouse gas emissions. The intermittency of renewable energy, the logistics and energy penalties of CO_2 capture and sequestration (CCS) pose major problems that prevent these technologies from being economically viable on a large scale [1,2]. Large scale integration of wind and solar energy into the electrical grid requires a storage technology which can supply electricity on demand from these fluctuating sources [2]. Current CCS processes suffer from the fact that CO_2 absorption by corrosive liquids such as monoethanolamine solutions (MEA) as well as adsorption by solids such as alkaline metal oxides rely on a high temperature thermal swing for their regeneration. These operations constitute the large portion of the cost of CO_2 capture [3–5]. An additional challenge lies in the logistics and energy penalties of managing the concentrated CO_2 that must be transported to either an underground injection facility or a processing plant for conversion to useful products.

The use of synthetic fuels made from CO_2 as carriers for excess renewable electricity offers a solution to manage fluctuating output of renewable energy while mitigating CO_2 emissions [6]. Production of synthetic natural gas (SNG) from CO_2 and renewable H_2 (via Eq. (1)) is one promising option which has been demonstrated on an industrial scale in Audi motor company's "e-gas" facility in Werlte (Germany); this facility produces 1000 metric tons/year of SNG from concentrated CO_2 obtained from a nearby biogas plant [7,8]. We report dual-function materials (DFM) that offer a unique renewable energy storage solution by producing SNG directly from industrial flue gas (dilute CO_2), while eliminating the energy requirement, corrosion and transportation issues associated with CCS. The DFM contains a sorbent as well as a catalyst component, allowing it to both capture CO_2 and convert it to a fuel without an energy intensive thermal swing process. The DFM process utilizes H_2 produced via electrolysis using renewable electricity (wind, hydro, geothermal, and/or solar) to make synthetic natural gas via the methanation reaction shown in Eq. (1). SNG as an energy carrier has advantages over H_2 because it can easily be handled and transported via the existing natural gas pipeline infrastructure. Furthermore, by eliminating a thermal swing process, the conversion of CO_2 to SNG using DFMs constrains the energy input to only renewable sources (in the form of H_2), thus allowing the CO_2 capture and utilization processes to approach carbon neutrality. Hence DFMs can be used to devise a carbon recycling scheme within

* Corresponding author. Tel.: +1 212 854 6390.
E-mail address: rf2182@columbia.edu (R.J. Farrauto).

http://dx.doi.org/10.1016/j.apcatb.2014.12.025
0926-3373/

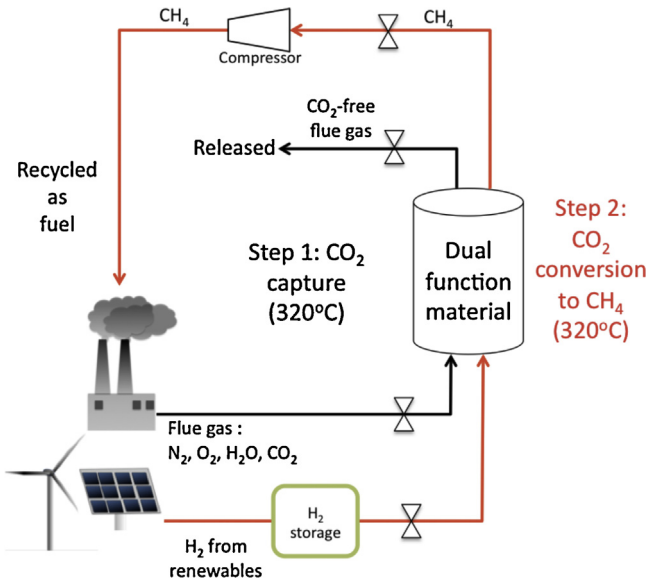

Fig. 1. Process diagram for CO_2 capture and recycle as synthetic natural gas (CH_4) back to an industrial facility. The CO_2 in the saturated adsorbent is methanated to SNG in the same reactor. This is shown as two separate process steps but they both occur in the same reactor and at the same temperature.

combustion (or fermentation) based industries while integrating more renewable energy into the grid.

The total dual function process for CO_2 capture and utilization (shown in Fig. 1) operates at a temperature of 320 °C, using heat recovered from the flue gas, thus eliminating the need for externally added energy. The DFM is housed inside one reactor, which adsorbs CO_2 until saturation and subsequently converts it to synthetic natural gas (SNG) catalytically. Stored H_2 (from renewable sources) is used to methanate the captured CO_2 according to Eq. (1). The resultant SNG + H_2O product is compressed, dried and the methane recycled to the front end of the process or the natural gas grid.

$$CO_2 + 4H_2 \rightarrow CH_4 + 2H_2O \Delta H = -164\,kJ/mol \quad (1)$$

A theoretical process where CO_2 is captured directly from ambient air using a K_2CO_3/Al_2O_3 composite sorbent and catalytically methanated at a higher temperature using renewable H_2 has been suggested in the literature [9]. In their publication, Veselovskaya et al. calculated the theoretical energy storage efficiency for their suggested process as 52%, based on energy requirements for thermal swing and water electrolysis [9]. This idea is also mentioned in the work by Derevschikov et al. which focuses on direct air capture using K_2CO_3/Y_2O_3 sorbents [10]. Xie et al. have developed and experimentally demonstrated the use of conjugated microporous polymers for CO_2 capture and subsequent conversion under ambient conditions to propylene carbonate, a chemical used in the pharmaceutical industry [11]. Yang et al. have reviewed the use of CO_2 as C_1 feedstock and suggested the direct conversion of captured CO_2 to commodity chemicals within amine based absorbent or adsorbents as a means of overcoming current problems associated with CCS [12]. Although the chemical conversion of CO_2 as a means to offset the costs of CO_2 capture has previously been considered in the literature, to our knowledge we present the first experimental demonstration of a simple isothermal CO_2 capture and methanation process that operates in a single reactor at the same temperature. Moreover, by producing synthetic natural gas our process ideally approaches carbon neutral power generation.

The conversion of CO_2 to methane has recently attracted attention as a means of reducing the emission of CO_2 from combustion sources to the atmosphere. The methanation reaction is well known and has recently been studied with particular emphasis on greenhouse gas mitigation and renewable energy storage [13–16]. In our previous work we have investigated CO_2 methanation over a Ru/γ-Al_2O_3 catalyst, which has shown excellent activity, stability and selectivity to CH_4 [16].

Since synthetic natural gas is produced through the exothermic CO_2 methanation reaction (Eq. (1)), it supplies the necessary energy for CO_2 desorption from the sorbent component of the DFM. Hence when the DFM is saturated with CO_2 and exposed to H_2, a spillover process occurs, which drives the chemisorbed CO_2 to catalytic sites for further methanation. In this way the DFM is regenerated at the end of each cycle. Dual function materials consisting of Ru as the catalyst and CaO as the adsorbent were prepared using the incipient wetness impregnation technique, which is a typical method for preparing catalyst materials in a highly dispersed state.

CO_2 chemisorption is expected to occur on both CaO and reduced Ru^0 sites in the DFM. However, chemisorption on Ru sites is negligible in the oxidizing environment of a power plant since Ru will not remain in its reduced state. In this case CO_2 reversibly chemisorbs on CaO sites. Upon the addition of H_2, spillover to Ru sites occurs via desorption of CO_2 from CaO sites and subsequent chemisorption of CO_2 on Ru sites. This is followed by catalytic methanation over Ru sites and desorption of products.

DFMs consisting of a combination of 1–11% Ru (by weight) and 1–10% CaO (by weight) dispersed on γ-Al_2O_3 carrier were investigated. Our previous work has shown that CaO dispersed on γ-Al_2O_3 (CaO/γ-Al_2O_3) behaves radically different compared to bulk or unsupported CaO. Its dispersion creates nano-sized islands of CaO, which are able to reversibly chemisorb CO_2 and therefore capture and release it at moderate temperatures (~300 °C) compared to bulk CaO, which forms carbonates that decompose at ~800 °C [17,18]. It is a critical advantage that reversible adsorption/desorption of CO_2 and methanation occur at the same temperature with these materials. Supported Ru is a suitable methanation catalyst achieving equilibrium conversions of CO_2 to CH_4 at 280 °C at a gas hourly space velocity of 4720 h^{-1}, [16]. Hence the components of the DFM are compatible at our operating temperature of 320 °C. While Ni is also a good methanation catalyst, it requires pre-reduction at temperatures greater than 400 °C in order to become active for CO_2 methanation [19–21] and hence is less suitable compared to Ru for cyclic oxidizing (CO_2 capture from flue gas) and reducing (methanation) conditions as required in this process.

2. Experimental

2.1. Material synthesis

Dual function materials were prepared by incipient wetness impregnation of either $Ru(NO)(NO_3)_2$ on 10 wt.% CaO/γ-Al_2O_3 or of $Ca(NO_3)_2$ on 10 wt.% Ru/γ-Al_2O_3. Detailed preparation procedures for CaO/γ-Al_2O_3 [18] and Ru/γ-Al_2O_3 [16] can be found in our previous work. All samples were dried in air at 120 °C for 1 h and calcined in air at 320 °C for 2 h. This pretreatment ensured the decomposition of $Ru(NO)(NO_3)_2$ to Ru. The DFMs received in-situ pre-reduction in 4% H_2/N_2 at 320 °C for 2 h at the beginning of each reactor test to ensure decomposition of $Ca(NO_3)_2$ to CaO.

2.2. Reactor testing of various DFM compositions using the Quantachrome chemisorption unit as microreactor

These tests were performed in a ChemBET Pulsar TPR/TPD unit (Quantachrome). Approximately 100 mg of powdered dual function material was loaded onto a quartz U-tube and then placed in the micro-reactor furnace (Quantachrome unit). The sample was

first reduced for 2 h at 320 °C in 4% H_2/N_2 (flow rate of 26 mL/min). This ensured that all the precursor salts (Calcium nitrate and Ruthenium(III) nitrosyl nitrate) decomposed to CaO and Ru, and at the same time ensured that any RuO_x species were reduced to Ru^0.

The sample was then exposed to a 10% CO_2/N_2 mixture (30 mL/min) at 320 °C for 30 min. This constituted the "CO_2 capture" step. Following this was a "methanation" step, which consisted of 4% H_2/N_2 (26 mL/min) being introduced into the reactor for 2 h. Online monitoring of gas compositions at the exit of the reactor was performed using an Enerac portable emissions analyzer, capable of continuously monitoring CO_2 and CH_4 concentrations. Sampling time of the Enerac was 1 s. Following the hydrogenation cycle the reactor was cooled to room temperature in He. It was observed that the measurements during the CO_2 capture step were unreliable due to the fact that measured CO_2 concentration differences were much smaller than the error in measurement (~4%) of the Enerac's CO_2 detector. Hence DFM performances were judged based on the amounts of methane released, which could be measured precisely, with only 4 ppm error.

2.3. Accelerated cyclic testing in a packed bed reactor

Powder 5% Ru,10% CaO/γ-Al_2O_3 was packed inside a quartz tube housed in a furnace. Gas analysis was performed on-line via an Enerac, which is an IR based gas analyzer for combustion applications. The DFM was pre-reduced in-situ at 320 °C for 2 h using 5% H_2/N_2 (46.3 mL/min). Cyclic tests were all performed at 320 °C. Each cycle consisted of a CO_2 capture step and a methanation step.

In the first cyclic test the CO_2 capture capability of 1.001 g of 5% Ru, 10% CaO/γ-Al_2O_3 from a source of 10% CO_2/air over 20 cycles of CO_2 capture and methanation was evaluated. Ruthenium (Ru) will oxidize when exposed to air in the capture mode and will subsequently be reduced during methanation. A feed gas of 90% air (~18% O_2) is well in excess of the 6–8% O_2 in a power plant effluent and thus this test should be considered accelerated test to stress the materials. During CO_2 capture 10% CO_2/air was introduced to the reactor at a flow rate of 17.4 mL/min for 20 min. The reactor was then purged with He until CO_2 and O_2 could no longer be detected at the exit. This was followed by methanation, which involved flowing 5% H_2/N_2 at 89.5 mL/min for 20 min. A dilute source of H_2 was used in order to prevent methane formation from exceeding our limits of detection; pure H_2 would be used in a stoichiometric amount relative to CO_2 captured in a power plant application. The cyclic experiment was performed with the same volume of γ-Al_2O_3 as a background test. Methanation was not observed during the test with γ-Al_2O_3.

A second 20 cycle test of CO_2 capture and methanation was performed in a flow reactor in order to evaluate the performance of our dual function material (DFM) 5% Ru 10% CaO/γ-Al_2O_3 upon exposure to a high concentration of steam present in flue gas. 1.0344 g of powder DFM (5% Ru 10% CaO/γ-Al_2O_3) was housed inside a quartz tube encased by the furnace. The feed gas mixture of 8% CO_2/21% H_2O/air (22.1 mL/min) was introduced to the reactor through a heated line. Because steam is known as a sintering aid the amount used in this test is in excess of what would be expected (6–8%) in a real power plant application, and thus the test conditions should be viewed as accelerated aging of the material. A cold trap immersed in an ice bath was added to the furnace exit to condense out water prior to Enerac analysis. The reactant gas mixture was preheated to a temperature that fluctuated between 195 and 200 °C before entering the furnace, which was always at 320 °C. Steam was generated by injecting distilled water via a syringe pump (KD scientific) into this preheating zone. For cycles 1–4, the preheating zone was kept at 130 °C. Methanation was performed after CO_2/H_2O/air flow was discontinued and the reactor purged with He. During methanation 5% H_2/N_2 mixture was introduced to the reactor at a flow rate of 90.5 mL/min. CO_2 capture and methanation durations were 45 min each.

2.4. Ru and CaO dispersion by H_2 and CO_2 chemisorption

Chemisorption experiments were performed using a ChemBET Pulsar TPR/TPD unit (Quantachrome). The fresh or cycled 5% Ru 10% CaO/γ-Al_2O_3 sample was placed inside the U shaped sample holder of the ChemBET Pulsar TPR/TPD unit and degassed to remove any vapors in the sample. Subsequently, the sample was reduced in-situ, in 4% H_2/N_2 (60 mL/min) at a temperature of 320 °C for 2 h. Following reduction, the sample was cooled to room temperature in helium. H_2 or CO_2 (both 100% purity) chemisorption of pretreated samples were performed at RT. CO_2 chemisorption was also performed on a sample of γ-Al_2O_3 to correct dispersion measurements for CO_2 which may be adsorbed on the support. It was assumed that each CO_2 adsorbed on one Ru site. It was assumed that H_2 chemisorption takes place only on Ru sites and that each H_2 molecule occupies 2 Ru sites. CO_2 chemisorption was used to calculate the total Ru and CaO sites, as well as sites associated with the support. CaO dispersions were calculated by subtracting from the total number of sites those of Ru (determined by H_2 chemisorption) and support sites (determined by CO_2 chemisorption on γ-Al_2O_3).

2.5. Temperature programmed desorption (TPD)

TPD was performed using a ChemBET Pulsar TPR/TPD unit (Quantachrome). The sample was heated from room temperature to a final temperature of 1000 °C in a flow of helium (100 mL/min) with a heating rate of 5 °C/min. The thermal conductivity of gases released from the sample was measured via a thermal conductivity detector (TCD). A cold trap placed upstream from the TCD was used to condense any water coming off of the sample. A calibration was performed separately where known volumes of CO_2 were injected (at room temperature) and TCD signals recorded. This calibration data were used to convert the thermal conductivity signal (in units of mV) to volume of CO_2 released. The TCD used for these experiments is capable of measuring thermal conductivity with less than 1% relative error.

3. Results and discussion

3.1. Reactor testing of various DFM compositions

Nine DFMs, as well as a 10% Ru/γ-Al_2O_3 methanation catalyst, were tested in a microreactor where cycles of CO_2 capture and methanation were performed. Methanation of captured CO_2 yielded a characteristic peak of methane observed at the exit of the reactor. The extents of methanation for each material are compared in Table 1. Table 1 displays the methanation capacity (g-mol

Table 1
Methane turnover (moles CH_4 produced/moles Ru present in sample) and methanation capacity (g-mol CH_4/kg DFM) for all samples during 1 cycle consisting of a CO_2 capture and a methanation step.

Row	Sample	CH_4/Ru	g-mol CH_4/kg DFM
1	γ-Al_2O_3	0.00	0.00
2	10% Ru/γ-Al_2O_3	0.10	0.10
3	1% CaO 10% Ru/γ-Al_2O_3	0.19	0.19
4	5% CaO 10% Ru/γ-Al_2O_3	0.27	0.27
5	10% CaO 10% Ru/γ-Al_2O_3	0.31	0.30
6	1.1% Ru 10% CaO/γ-Al_2O_3	2.46	0.27
7	2% Ru, 10% CaO/γ-Al_2O_3	1.79	0.35
8	5% Ru 10% CaO/γ-Al_2O_3	1.01	0.50
9	6.8% Ru,10% CaO/γ-Al_2O_3	0.65	0.44
10	10.6% Ru, 10% CaO/γ-Al_2O_3	0.44	0.46
11	10% Ru/γ-Al_2O_3 +10% CaO/γ-Al_2O_3	0.25	0.12

CH_4/kg DFM) and the methane turnover (g-mol CH_4/g-mol Ru in DFM) of all samples tested in the microreactor. It can be seen from rows 3–5 in Table 1 that the addition of CaO to 10% Ru/γ-Al_2O_3 results in increased methane production; 10% CaO 10% Ru/γ-Al_2O_3 produces 3 times as much CH_4 as 10% Ru/γ-Al_2O_3. CO_2 methanation is not observed on CaO/γ-Al_2O_3 only. This is a clear demonstration of the operation of dual function materials; CO_2 adsorbs on both CaO and reduced Ru sites during CO_2 capture. Upon introduction of H_2, methanation begins with the CO_2 chemisorbed on Ru sites and releases heat, which drives CO_2 desorption from the nano dispersed CaO sites resulting in further methanation.

Rows 6–10 in Table 1 display methanation results for materials prepared by impregnating 1–10% Ru on 10% CaO/γ-Al_2O_3. It is apparent from Table 1 that all such samples performed significantly better compared to our original catalyst (10% Ru/Al_2O_3) based on methane production. As indicated by the CH_4/Ru column the greatest amount of spillover of CO_2 occurs in the sample containing 1.1% Ru and 10% CaO. However, it is the 5% Ru, 10% CaO sample that shows the largest production of CH_4 per kg of material. This indicates that a large CaO:Ru ratio in the DFM is desirable since it increases the amount of methanation. However, low loadings of Ru do not generate sufficient heat to liberate all CO_2 from CaO sites, which likely causes the overall methanation capacity to be lower for the 1.1% Ru 10%, CaO/Al_2O_3 compared to the 5% Ru, 10% CaO/Al_2O_3.

In order to determine whether the order in which the Ru and CaO were loaded onto the γ-Al_2O_3 support affect the methanation performance of the different materials, the sample containing 10% CaO impregnated on 10% Ru/Al_2O_3 (row 5 of Table 1) was compared with the sample containing 10.6% Ru impregnated on 10% CaO/Al_2O_3 (row 10 of Table 1). A physical mixture of equal parts 10% Ru/γ-Al_2O_3 and 10% CaO/γ-Al_2O_3 was tested and compared with these samples to determine whether the co-impregnation of CaO and Ru gave any additional benefits over the physical mixture. When comparing this to the other samples, CH_4/Ru, which is a measure of CO_2 spillover will be the focus of the discussion. It can be seen from Table 1 that the performance is significantly enhanced when Ru is impregnated onto the CaO/γ-Al_2O_3. This is also verified by the increased methane production per Ru sites (CH_4/Ru) shown in Table 1. One possible explanation for this is that CaO impregnation on Ru/γ-Al_2O_3 results in some loss of active Ru sites due to masking by the CaO of the Ru. Another possibility is that the presence of CaO on the support during Ru impregnation results in increased dispersion of the Ru in the final DFM. This phenomenon has recently been observed by Munera et al. for Rh impregnated on CaO/SiO_2 supports, although for samples with much higher concentrations of CaO in the support (20–50 wt.%) and much lower Rh loadings (0.6 wt.%) [22]. However, any effects of increased dispersion, while likely, are only secondary to those resulting from spillover of CO_2 from CaO to Ru sites; this is clearly observed when comparing the methane turnover of 10% Ru/γ-Al_2O_3 (Table 1, row 2) with those of samples containing 1–10% CaO impregnated on 10% Ru/γ-Al_2O_3 (Table 1, rows 3–5) and the physical mixture of 10% CaO/γ-Al_2O_3 with 10% Ru/γ-Al_2O_3 (Table 1, row 11). Significant enhancement of methanation capacities are observed in all these cases where CaO cannot have an impact on Ru dispersion, compared to the 10% Ru/γ-Al_2O_3 baseline.

While impregnation of Ru on CaO/γ-Al_2O_3 results in the best observed methanation activity, other synthesis methods can be explored in the future. The physical mixture of 10% Ru/γ-Al_2O_3 and 10% CaO/γ-Al_2O_3 (row 11) showed increased methanation per kg as well as per mole of Ru present in sample compared to the 10% Ru/γ-Al_2O_3, clearly demonstrating that the spillover mechanism proposed is effective regardless of any surface interactions between Ru and CaO. However, the methane produced per Ru site was better for the samples where CaO and Ru were both deposited on the same γ-Al_2O_3 support. This shows that proximity of CaO and Ru sites plays an important role on the performance of DFMs, also consistent with a CO_2 spillover mechanism from the CaO to the Ru.

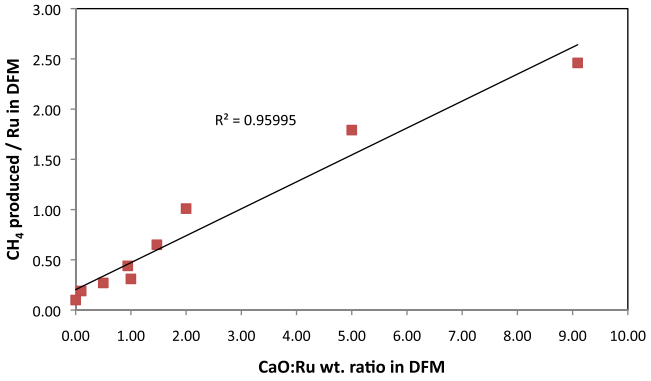

Fig. 2. Methane turnover for varying CaO:Ru (weight ratio) in the sample.

Based on results shown in Table 1, the sample exhibiting the largest methanation activity per kg is 5% Ru, 10% CaO/γ-Al_2O_3 shown as row 8. This sample produced five-times as much methane as our original methanation catalyst, 10% Ru/Al_2O_3 (row 2). Hence it was chosen as a candidate for advanced testing. The best performance was obtained when the Ru precursor salt was impregnated onto the CaO dispersed on the γ-Al_2O_3. This is shown when rows 10 and 3, 8 and 4 are compared. It is also noted that co impregnated samples (row 10) performed better than mechanical mixtures of the same amount of Ru and CaO but on separate particles (row 11).

Although the methanation activity is highest for 5% Ru, 10% CaO/γ-Al_2O_3, it can be seen from Table 1 that the highest methane turnover (CH_4/Ru) is observed for 1% Ru, 10% CaO/γ-Al_2O_3. In fact, when the methane turnover is plotted against the weight ratio of CaO to Ru in the material (CaO:Ru) as in Fig. 2, a direct correlation is observed. Thus CO_2 spillover from CaO to Ru sites increases with the increasing weight ratio of CaO to Ru. This suggests that individual Ru sites generate more methane due to migration of CO_2 from CaO to Ru. The extent of CO_2 spillover from CaO to Ru sites increases greatly by increasing the CaO content for a given amount of Ru.

3.2. *Accelerated cyclic testing under post-combustion conditions: CO_2 capture from highly oxidizing streams*

The sample demonstrating largest methanation activity per kg DFM (5% Ru, 10% CaO/γ-Al_2O_3) was chosen for further evaluation under more realistic post combustion conditions. In a real post-combustion CO_2 capture application the DFM will have to capture CO_2 in the presence of air over many cycles of operation; a natural gas fired turbine generates a flue gas containing 3–4 vol.% CO_2 and (12–15%) O_2 [3]. Post combustion flue gas will also contain steam (6–8% in the case of the natural gas fired turbine). Hence in order to understand the effect of power plant conditions on the performance of DFMs, two cyclic tests were performed using 5% Ru,10% CaO/γ-Al_2O_3. The first cyclic test involved CO_2 capture in the presence of air to investigate the impact of oxygen on the CO_2 capture and hydrogenation performance of the DFM. It also tests the resilience of Ru during redox (reducing and oxidizing) cycles. A second cyclic test (performed with fresh DFM) was performed with CO_2 capture from a mixture containing air, steam and CO_2 to simulate further a power generation effluent. The response of the components of the DFM to oxidizing conditions is a crucial piece of information gathered from these cyclic studies.

Cyclic tests with air (~18% O_2) present were performed from a source of 10% CO_2/air over 20 cycles of CO_2 capture and methanation in a packed bed reactor. Note that O_2 concentration in this test is above that expected in the effluent and thus can be considered

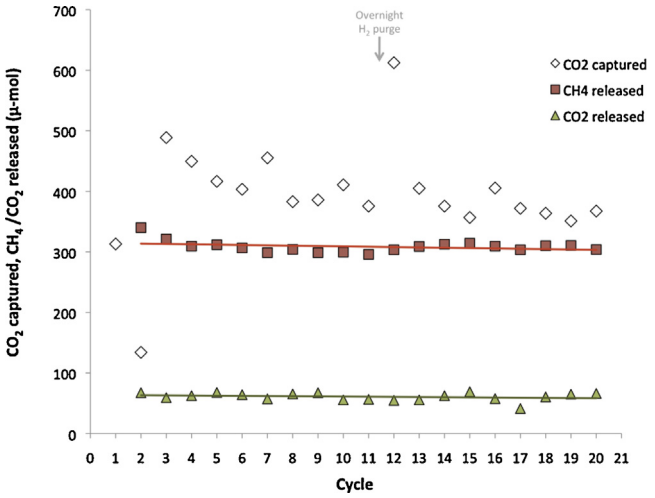

Fig. 3. CO_2 captured, CH_4 released and CO_2 released for 20 cycles of methanation. One cycle consists of CO_2 capture from a 10% CO_2/air stream for 20 min followed by a He purge and subsequent 20 min methanation by flowing 5% H_2/N_2. $T = 320\,^{\circ}C$. An overnight purge with 5% H_2/N_2 was performed after the 11th cycle.

an accelerated test. The results are displayed in Fig. 3. The hollow diamond points indicate CO_2 capture during the first step of the cycle, and the filled square and triangle data points indicate the CH_4 and CO_2 released during the methanation step associated with each cycle. Due to a mass flow controller related error in the first cycle the first reliable data is from the methanation step in the 2nd cycle. A stable CO_2 and CH_4 release is observed during methanation in the subsequent 19 cycles. However, there is variability in the CO_2 captured during each cycle, which shows a slightly decreasing trend up to cycle 11. After the 11th cycle, the reactor was purged with 5% H_2/N_2 overnight at 320 °C to see whether this would restore CO_2 capture activity and increase methanation activity by releasing all CO_2 remaining in the DFM. As can be seen from Fig. 3, this resulted in a significant increase in the CO_2 captured during cycle 12, without any proportional change in the amounts of CH_4 and CO_2 released. This means that while the overnight H_2 purge freed some sites for CO_2 capture, CO_2 molecules are more strongly bound to these sites and are only slowly removed during methanation. A longer methanation period regenerates those sites. Overall, stable methanation activity was observed for 19 cycles.

A detailed analysis of results from cyclic experiments performed with 5% Ru 10% CaO/γ-Al_2O_3 is displayed in Table 2. It includes the CO_2 capture capacity, conversion of captured CO_2 to CH_4, and the gas phase carbon balance for each cycle. The average carbon balance based on measured gas concentrations for cycles 3–20 was 91.23%. This indicates that most of the CO_2 adsorbed is reversibly released from the material. Thus about 9% of the CO_2 remains on sorbent (CaO) sites. Nevertheless, we do not see a significant change in amounts of CO_2 or CH_4 released from the DFM over 19 cycles (as seen in Fig. 3), which implies that accumulation of carbon on the surface of the DFM does not take place to an appreciable extent. When 100% H_2 is used in the real application it is expected that most, if not all of these sites, will lead to the formation of CH_4. This method also can be used to achieve a more favorable carbon balance. The average conversion of captured CO_2 to CH_4 was 76.17% over 19 cycles. This is comparable to the results by Rynkowski et al. using 5% Ru/γ-Al_2O_3 where a maximum CO_2 conversion of 72% was observed around 400 °C using a mixture of H_2/CO_2 (5:1 volumetric ratio) [23]. Most of the remaining CO_2 is released as a result of the heat generated during methanation, and can be converted to methane in a small downstream catalytic reactor to upgrade the mixture to pure CH_4. The downstream reactor will likely operate at a lower temperature to achieve more favorable equilibrium conversions. We have already shown that 10% Ru/γ-Al_2O_3 allows us to reach equilibrium conversions at 280 °C [16]. The average CO_2 capture capacity was 0.41 g-mol CO_2/kg DFM and the average methanation capacity was 0.31 g-mol CH_4/kg DFM over 19 cycles.

Table 2
Detailed analysis of the 20 cycle test performed on 5% Ru, 10% CaO/γ-Al_2O_3. One cycle consists of CO_2 capture from a 10% CO_2/air stream for 20 min followed by a He purge and subsequent 20 min methanation by flowing 5% H_2/N_2. $T = 320\,^{\circ}C$. An overnight purge with 5% H_2/N_2 was performed after the 11th cycle.

Cycle	CO_2 captured (mL)	CH_4 released (mL)	CO_2 released (mL)	CO_2 captured (μ-mol)	CH_4 released (μ-mol)	CO_2 released (μ-mol)	Gas phase C balance (%)	Conversion to methane (%)	CO_2 capture capacity (g-mol/kg)
1	7.7	NA	NA	313.1	NA	NA	NA	NA	0.3
2	3.3	8.3	1.7	134.1	340.1	67.4	304.0	253.7	0.1
3	12.0	7.9	1.5	488.8	321.3	59.3	77.8	65.7	0.5
4	11.0	7.6	1.5	449.6	309.4	62.5	82.7	68.8	0.4
5	10.2	7.6	1.7	416.5	311.9	67.8	91.2	74.9	0.4
6	9.9	7.5	1.6	403.4	306.6	64.2	91.9	76.0	0.4
7	11.1	7.3	1.4	455.3	298.8	57.2	78.2	65.6	0.5
8	9.4	7.4	1.6	383.0	304.1	65.4	96.5	79.4	0.4
9	9.4	7.3	1.7	385.8	298.8	67.4	94.9	77.4	0.4
10	10.1	7.3	1.4	410.8	299.6	55.6	86.5	72.9	0.4
11	9.2	7.2	1.4	375.6	295.9	56.4	93.8	78.8	0.4
12	15.0	7.4	1.3	612.4	303.5	54.8	58.5	49.6	0.6
13	9.9	7.6	1.4	405.1	309.0	55.6	90.0	76.3	0.4
14	9.2	7.7	1.5	375.6	312.7	62.5	99.9	83.2	0.4
15	8.7	7.7	1.7	356.8	314.3	69.1	107.4	88.1	0.4
16	9.9	7.6	1.4	405.5	309.4	57.6	90.5	76.3	0.4
17	9.1	7.4	1.0	371.9	303.5	41.3	92.7	81.6	0.4
18	8.9	7.6	1.5	363.8	310.2	60.5	101.9	85.3	0.4
19	8.6	7.6	1.6	351.1	310.6	65.0	107.0	88.5	0.4
20	9.0	7.4	1.6	367.5	303.9	66.2	100.7	82.7	0.4

Table 3
Characterization of 5% Ru 10% CaO/γ-Al_2O_3 before and after 20 cycles of CO_2 capture and methanation at 320 °C.

Sample	Ru dispersion (%)	CaO dispersion (%)	BET surface area (m^2/g)
Fresh DFM (5% Ru 10% CaO/γ-Al_2O_3)	26.3	13.6	83.9
DFM after 20-cycle test with simulated dry flue gas	21.0	10.0	92.7
DFM after 20-cycle test with simulated wet flue gas	20.1	1.7	89.0

There is a need to improve the CO_2 capture capacity of the DFM, as it is low compared to those of other state of the art CaO based sorbents that have been evaluated for post-combustion CO_2 capture (>2 g-mol CO_2/kg sorbent) [24]. One way of increasing CO_2 capture capacity would be by increasing the CaO loading on γ-Al_2O_3. However, it has previously been demonstrated that the reversibility of chemisorption depends on the presence of nano-sized CaO particles, which means that there will be a tradeoff between reversibility of adsorption and capture capacity [17,18]. For this reason, promoters and other sorbents suitable for operation under catalytic reaction conditions are also being investigated.

In order to evaluate the performance the 5% Ru 10% CaO/γ-Al_2O_3 upon exposure to steam, another cycle test was performed where the simulated flue gas used for CO_2 capture cycles consisted of 8% CO_2, 21% H_2O, and balance air. The concentration of steam in this test far exceeds what would be typical for a natural gas (methane) power plant (6–8%) and thus constitutes an extreme oxidizing/sintering condition for the use of DFMs. The results showing CH_4 and CO_2 released during each methanation cycle are plotted in Fig 4. For this experiment, the background measurements for the CO_2 capture cycles (using γ-Al_2O_3) showed significant variation in residence time of the flue gas in the reactor, which has prevented the accurate measurement of CO_2 captured during the cycle test. This is attributed to the fluctuating flow rate of steam due to the use of a syringe pump for its generation (see Section 2). However, the CH_4 and CO_2 released can be used to understand the effect of high concentrations of steam on this system. While an overnight H_2 purge was also performed after the 11th cycle of this test, it did not result in a significant change in methane production. CH_4 produced during methanation portions of these cycles fluctuates around a mean value of 283 μ-mol, which translates to an average methanation capacity of 0.27 g-mol CH_4/kg DFM, about 10% lower than in the absence of steam (0.31 g-mol CH_4/kg DFM over 19 cycles). While this may not be a significant difference, the composition of the gas released during methanation has changed in a positive direction in that very little CO_2 was detected with 99.9% methane released on average. In no cases was CO present. In the absence of steam, methanation produced a gas mixture containing on average 83.6% CH_4 and 16.4% CO_2 by volume. The increased purity of methane released creates the advantage of simplicity in overall process design. A high purity methane yield will eliminate the need for downstream catalytic treatments to prepare the gas for injection to natural gas pipelines.

Fresh 5% Ru, 10% CaO/γ-Al_2O_3 and spent DFM samples from both cyclic tests were characterized via BET surface area analysis as well as H_2 and CO_2 chemisorption to determine Ru and CaO dispersions. The dispersion values indicate the percentage of Ru or CaO actively participating in CO_2 adsorption or catalysis. Results shown in Table 3 indicate that BET surface area has not been affected as a result of aging cycle tests, The dispersions of both Ru and CaO (also shown in Table 3) decrease by no more than 20% after 20 cycles of CO_2 capture and methanation, when the simulated flue gas only contains air and CO_2. Where steam was present, the Ru dispersion was similar to that after the test with air only (about 24% lower than fresh). However, the CaO dispersion is greatly reduced; the dispersion of CaO drops by 87% after the cyclic test with steam.

Although CaO dispersion of the DFM shows a significant decrease after the accelerated cycle test involving steam, the methanation capacity is not drastically affected. Furthermore, in Fig. 4 the amount of methane produced does not show a significant decreasing trend over time. One explanation is that the DFM contained a number of excess or "inactive" CaO sites in the fresh state and losing those sites did not affect material performance during the test. When compared to the values presented in Table 1, methanation capacity of 5% Ru, 10% CaO/γ-Al_2O_3 is lower for both cycle tests compared to the measurements made in the absence of oxygen or steam. This can easily be attributed to some oxidation of Ru. However, the methanation capacities for both cycle tests are nevertheless much higher than that of 10% Ru/γ-Al_2O_3 (Table 1, row 2) which indicates that the methanation is still being enhanced by the presence of CaO.

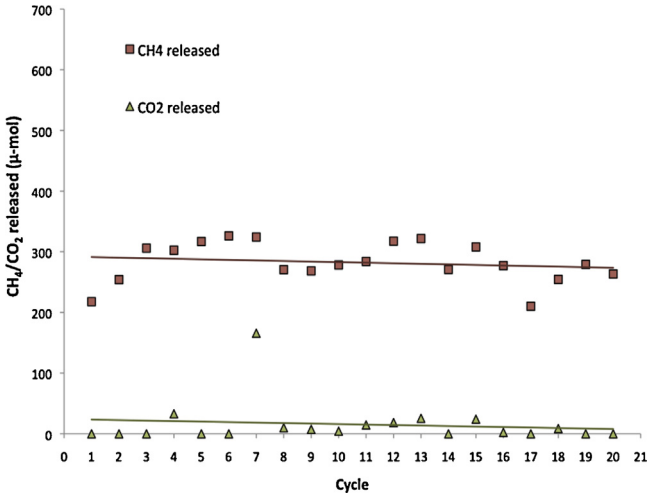

Fig. 4. CH_4 and CO_2 released upon H_2 introduction during the 20-cycle test with steam exposure. Feed during CO_2 capture: 8% CO_2/21% H_2O/air (22.1 mL/min), Feed during H_2 introduction: 5% H_2/N_2 (90.5 mL/min).

Temperature programmed desorption (TPD) was performed on the spent DFM sample thinking that perhaps some carbonate had formed leading to a lower CO_2 chemisorption. The TPD results showed that a total of 7.7201 μ-mol of CO_2 were remaining on a 0.1001 g sample (77.1240 μ-mol/g). However, CO_2 desorption is observed only below 60 °C, which indicates that these are weakly adsorbed molecules taken up by the sample after it was removed from the reactor. Since no carbonate decomposition was observed the decrease in CaO dispersion is attributed to sintering mainly due to the accelerated test with 21% steam. It is therefore necessary to understand the rate of CaO sintering in the presence of the more realistic 6–8% steam in the flue gas. Further feasibility studies to understand mechanisms and rates of deactivation of DFMs over prolonged periods of testing under realistic conditions will be the subject of future experimentation.

4. Conclusions

A combined adsorbent and catalyst (dispersed CaO and Ru) operating at the same temperature in the same reactor captures CO_2 in the presence of air and steam. The addition of stored renewable H_2 (from renewable electricity) produces synthetic natural gas at high efficiencies. The synthetic natural gas can then be recycled to an industrial facility, conserving fuel while minimizing CO_2 release. This feasibility study represents a major departure from carbon capture and sequestration technology currently being investigated for decreasing green-house gas emissions.

For samples containing equal amounts of Ru, the addition of CaO increased methane yield, demonstrating that CO_2 spillover from CaO to Ru sites is occurring in DFMs. It was observed that increasing CaO:Ru ratio results in a greater extent of spillover of CO_2 and hydrogenation to CH_4. However there is an optimum composition around 5% Ru, 10% CaO/γ-Al_2O_3. Impregnation of Ru on CaO/γ-Al_2O_3 results in better performance compared to materials where CaO is impregnated on Ru/γ-Al_2O_3. 5% Ru, 10% CaO/γ-Al_2O_3 was tested under simulated post combustion conditions where CO_2 capture was performed from a dry gas mixture consisting of 10% CO_2 in air and under accelerated aging conditions using a mixture

consisting of 8% CO_2/21% H_2O/air. DFM showed stable methanation performance over both cyclic tests with up to 99.9% methane purity obtained in the cycle test where steam was present during CO_2 capture.

Acknowledgments

We wish to thank BASF for their generous financial support and encouragement.

References

[1] P. Folger, Carbon Capture and Sequestration: Research, Development, and Demonstration at the U.S, in: C.R. Service (Ed.), Department of Energy, 2014.
[2] A. Evans, V. Strezov, T.J. Evans, Renewable Sustainable Energy Rev. 16 (2012) 4141–4147.
[3] A. Samanta, A. Zhao, G.K.H. Shimizu, P. Sarkar, R. Gupta, Ind. Eng. Chem. Res. 51 (2012) 1438–1463.
[4] D.Y.C. Leung, G. Caramanna, M.M. Maroto-Valer, Renewable Sustainable Energy Rev. 39 (2014) 426–443.
[5] P.A. Webley, Adsorption 20 (2014) 225–231.
[6] G. Centi, E.A. Quadrelli, S. Perathoner, Energy Environ. Sci. 6 (2013) 1711–1731.
[7] Energy Turnaround in the Tank, Audi, 2014. www.audi.com, http://www.audi.com/com/brand/en/vorsprung_durch_technik/content/2013/10/energy-turnaround-in-the-tank.html
[8] P.F. Tropschuh, E. Pham, Sustainable automotive technologies, in: Proceedings of the 5th International Conference ICSAT 2013, Springer International Publishing, 2013, pp. 185–190.
[9] J.V. Veselovskaya, V.S. Derevschikov, T.Y. Kardash, O.A. Stonkus, T.A. Trubitsina, A.G. Okunev, Int. J. Greenhouse Gas Control 17 (2013) 332–340.
[10] V.S. Derevschikov, J.V. Veselovskaya, T.Y. Kardash, D.A. Trubitsyn, A.G. Okunev, Fuel 127 (2014) 212–218.
[11] Y. Xie, T.-T. Wang, X.-H. Liu, K. Zou, W.-Q. Deng, Nat. Commun. 4 (2013) 1–7.
[12] Z.-Z. Yang, L.-N. He, J. Gao, A.-H. Liu, B. Yu, Energy Environ. Sci. 5 (2012) 6602–6639.
[13] I. Graca, L.V. Gonzalez, M.C. Bacariza, A. Fernandes, C. Henriques, J.M. Lopes, M.F. Ribeiro, Appl. Catal. B 147 (2014) 101–110.
[14] S. Tada, O.J. Ochieng, R. Kikuchi, T. Haneda, H. Kameyama, Int. J. Hydrogen Energy 39 (2014) 10090–10100.
[15] G. Garbarino, P. Riani, L. Magistri, G. Busca, Int. J. Hydrogen Energy 39 (2014) 11557–11565.
[16] C. Janke, M.S. Duyar, M. Hoskins, R. Farrauto, Appl. Catal. B 152–153 (2014) 184–191.
[17] P. Gruene, A.G. Belova, T.M. Yegulalp, R.J. Farrauto, M.J. Castaldi, Ind. Eng. Chem. Res. 50 (2011) 4042–4049.
[18] M.S. Duyar, R.J. Farrauto, M.J. Castaldi, T.M. Yegulalp, Ind. Eng. Chem. Res. 53 (2014) 1064–1072.
[19] G. Du, S.Y. Lim Yang, C. Wang, L. Pfefferle, G.L. Haller, J. Catal. (2007) 370–379.
[20] B. Mile, D. Stirling, M.A. Zammitt, A. Lovell, M. Webb, J. Catal. (1988) 217–229.
[21] C. Li, Y.-W. Chen, Thermochim. Acta (1995) 457–465.
[22] J. Munera, B. Faroldi, E. Frutis, E. Lombardo, L. Cornaglia, S.G. Carrazan, Appl. Catal. A (2014) 114–124.
[23] J. Rynkowski, T. Paryjczak, A. Lewicki, M.I. Szynkowska, T.P. Maniecki, W.K. Jozwiak, React. Kinet. Catal. Lett. 71 (2000) 55–64.
[24] J. Wang, L. Huang, R. Yang, Z. Zhang, J. Wu, Y.Q. Gao Wang, D. O'Hare, Z. Zhong, Energy Environ. Sci. (2014) 3478–3518.